A Gyroscopic Damper System
– Damping with New Characteristics

Bastian **Scheurich**
Karlsruhe Institute of Technology, Karlsruhe, Germany

Dr. Tilo **Koch**
AUDI AG, Ingolstadt, Germany

Dr. Michael **Frey**, Prof. Dr. Frank **Gauterin**
Karlsruhe Institute of Technology, Karlsruhe, Germany

Summary

A new approach substitutes the damper of a passenger car by a cardanic gimbaled flywheel mass. The constructive design leads to a rotary damper in which the vertical movement of the wheel carrier leads to revolution of the rotational axis of the flywheel. In this arrangement, the occurring precession moments are used to control damping moments and to store vibration energy. Different damper characteristics are achieved by different velocities of the inner ring. From almost zero torque output to high torque output, this damper has a huge spread. With this kinetic energy storage recuperated damping energy stays in the damping system and does not stress the cars electrical system.

1   Introduction

The standard approach for dissipating the vibrational energy of passenger car bodies is the use of telescopic hydraulic shock absorbers. A first aspect of such a damping concept is the linear acting principal. This damper claims a certain construction height and limits the required space of e.g. luggage space or tire scope. A second aspect is the fact that the hydraulic principal dissipates kinetic energy into heat.

In the state of the art there is no damper which works in rotational principal in a mass-production vehicle. Even if there is no mass-production damper with the capability to gain kinetic energy there are a lot research projects on this topic.

Scientifically proven is the fact that there is a possibility to gain energy from dampers. Papers like [1] and [2] identify a potential of up to 600 Watt per vehicle. But the exact amount of energy recuperation depends on the unevenness of the road. Different damping concepts try to gain this kinetic energy potential with a generator. Damping systems used in [3] and [4] use a mechanical gearbox to transform the vertical movement of the wheel carrier in a state of motion which is useful for an electrical generator. A fast rotation of the generator with a low torque is considered as useful because of manufactured size. Besides there are solutions like [5] which use a

hydraulic transmission to drive an electric generator. Other solutions without a transmission like [6] damp the movement with magnetic fields.

All mentioned concepts have disadvantages. A gear box transmits the inertia of the generator to a higher level and leads to a stiffer connection of the damper at high frequencies. The transformation from hydraulic to mechanical motion entails a loss of energy. The avoidance of a gear box has to be paid with manufactured size.

Next to applications from automotive engineering there are gyroscopic systems like [7] and [8] which gain energy from wave movement. In those systems a floating body follows the wave movement. The outer part of a two-axis cardanic gimbaled gyroscope follows the housing of the floating body. In the inner part the gyroscope rotates with high revolutions. The outer movement leads to a gyroscopic induced slewing. This is connected and damped with an electric generator.

Another example is [9]. In this paper oscillations of a ropeway get damped by a gyroscopic arrangement. A passive damping of the precession induced movement is shown. A widespread use of the gyroscopic effect is the roll stabilization of vessels like covered in [10].

A lot of systems with no or small contact to earth use the gyroscopic effect to support their own orientation. Additionally to stabilization the precession induced relative velocity can be used for recuperation. Altogether the gyroscopic systems deal with alternating motions and have little input torque of a generator with a huge output torque.

The requirements on a rotational damper are quite similar. The wheel carrier has alternating oscillations and a damping of the oscillations requires a high torque. Next the kinetic energy can be stored as electric energy instead of dissipate it to heat. Following it is obvious to establish the following research question.

Is it possible to use the gyroscopic effect as transmission to build a rotational damper which recuperates electric energy? Which advantages or disadvantages will follow from such integration?

In order to investigate this question this paper will serve as a proposal. A derivation of the gyroscope properties and a proposal for integration into the chassis are set at the beginning. In a simulation environment a quarter car is built and the gyroscopic damper is integrated. Further the gyroscopic damper is compared to a linear damper concept. In the end typical maneuver in a vertical dynamic investigation show the relevant characteristics.

If package and force creation make it suitable to get damper forces which are needed at each time by a passenger car, it is possible to introduce a gyroscopic damper system in a vehicle. Consequently a gyroscopic damper provides several benefits to a vehicle. First there is the capability of recuperation of kinetic energy of the vertical movement of the wheel carrier. Next there is a rotary construction realizable which

copes with new potentials regarding packaging. Next there is an inertia rotating with high angular velocity which could be used as energy storage.

2 Methods and Materials

Fig. 1 shows a cardanic gimbaled gyroscope. According to [11] we define the outer gimbal turning around z-axis. It is pivoted in the frame and has the rotating angle ψ. The inner ring rotates around y-axis. It is pivoted in the outer gimbal and the rotation angle is named θ. In the middle the rotating mass is pivoted in the inner ring and rotates around x-axis. Its name is φ. Three torques (M_ψ, M_θ and M_φ) are acting from outer to inner axis. As shown in Fig. 1 the motion of the gyroscope is defined by the mechanism from external z_G over y_G to internal x_G.

Assmann shows in [13] that in the body orientated coordinate system the motion of the body influence the torque $\vec{M}$ with

$$\vec{M} = \frac{d}{dt}(J \cdot \vec{\omega}) \tag{1}$$

In eq. (1) the body has the angular velocity $^3\vec{\omega}$ and the inertia tensor J:

$$J = \begin{bmatrix} J_\psi & 0 & 0 \\ 0 & J_\theta & 0 \\ 0 & 0 & J_\varphi \end{bmatrix} \tag{2}$$

In the system from Fig. 1 the rotational matrix $^0T_3$ with

$$^0T_3 = \begin{bmatrix} c\psi\, c\theta & -s\psi\, c\varphi + c\psi\, s\theta\, s\varphi & s\psi\, s\varphi + c\psi\, s\theta\, c\varphi \\ s\psi\, c\theta & c\psi\, c\varphi + s\psi\, s\theta\, s\varphi & -c\psi\, s\varphi + s\psi\, s\theta\, c\varphi \\ -s\theta & c\theta\, s\varphi & c\theta\, c\varphi \end{bmatrix} \tag{3}$$

transforms the body coordinate system in the initial coordinate system $^0K = {}^0T_3\, {}^3K$. To keep the notation clear sine and cosine are truncated to their first letter. Combined with eq. (1) the equation of motion for the torque M_ψ with

$$M_\psi = \left(2J_\psi - 2J_\varphi\right)\dot{\theta}\dot{\psi}\, s\theta\, c\theta - J_\psi\dot{\varphi}\dot{\theta}\, c\theta + \left(J_\varphi - J_\psi\right)\ddot{\psi}\, c\theta^2 - J_\psi\, s\theta\, \ddot{\varphi} + J_\psi\ddot{\psi} \tag{4}$$

is derived. A simplification of $J_\theta = J_\varphi$ is assumed.
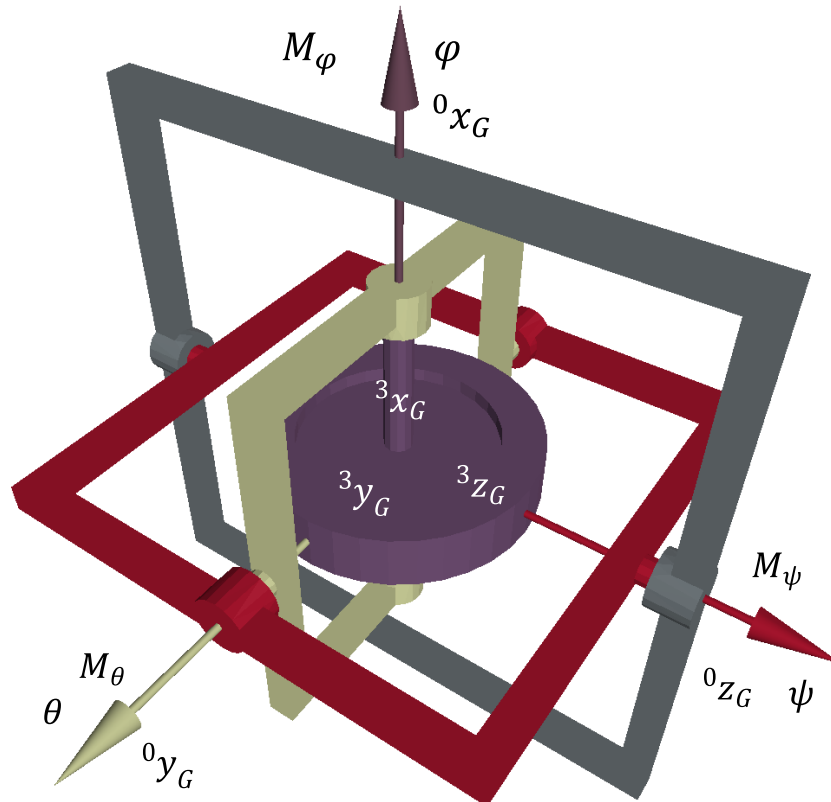
Fig. 1:   Basic principal of the gyroscopic arrangement.

In order to use the cardanic gimbaled gyroscope as a damper system, it is mounted in the chassis. A quarter car with a double wishbone wheel suspension is chosen. The principle arrangement of the gyroscope to the vehicle chassis is shown in Fig. 2. The frame of the gyroscope is mounted to the vehicle body. The outer gimbal is connected to the lower wishbone. Accordingly a movement of the lower wishbone around x_V turns the outer ring of the gyroscope around angle ψ. Obviously a vertical movement of the wheel carrier has direct influence on the dampers angle ψ. This disturbs the perpendicular directional vector of the angular velocity $\dot{\varphi}$. Induced by a precession torque the inner ring rotates around angle θ. If there is no M_θ acting against the rotation of $\dot{\theta}$ the torque M_ψ is very high because $\dot{\theta}$ has a high magnitude. To define the angular velocity $\dot{\theta}$ a certain torque M_θ is necessary. This torque is controlled by an electric motor. It is mounted on the outer gimbal and provides M_θ. Different damper characteristics are achieved by different velocities $\dot{\theta}$ of the inner gimbal. From almost zero torque output M_ψ to high torque output M_ψ, the spread depends on M_θ.

In the same way the described behavior of M_ψ follows from eq. (1). The torque M_ψ is mainly influenced by the angular velocity $\dot{\theta}$ and $\dot{\varphi}$. The intention of this paper is the use of M_ψ as a damper torque.
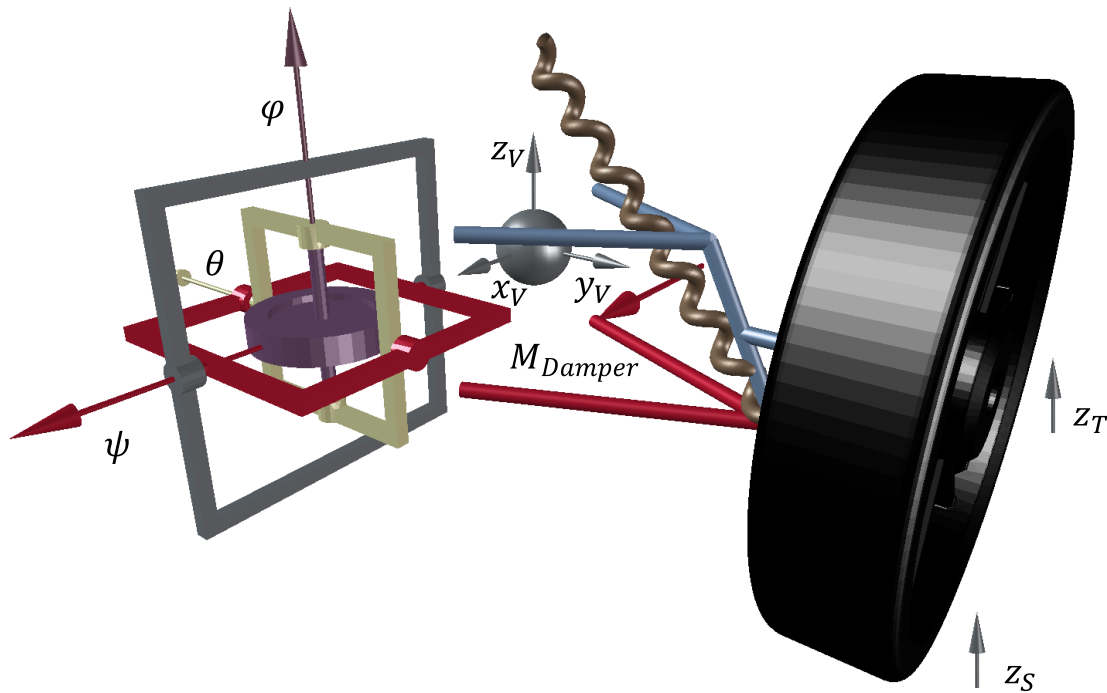
Fig. 2:   Quarter car model.

For the further investigation it is assumed that the lower wishbone has a length of $350\ mm$. Due to mounting position there is a mechanical ratio of 0.6 from ψ to the rotation of the lower wishbone around axis x_V. Since the vehicle itself is described in cardanic coordinate system of DIN70000 a rotation of the gyroscope's frame with $[\pi/2, -\pi/2, \pi/2]$ in ^0K_G was necessary.

For a given vehicle size and reasonable rotational speed a size for the turning mass was found with

$$J = \begin{bmatrix} 1 & 0 & 0 \\ 0 & 0.5 & 0 \\ 0 & 0 & 0.5 \end{bmatrix} \cdot 0.01\ [kg\ m^2] \tag{5}$$

A realization of J in real construction leads to Tab. 1.

Mass	$3\ [kg]$
Outer diameter of rotating inertia	$15\ [cm]$
Material	$Steel$

Tab. 1:   Data for the constructive realization of the rotating element.

The initial angular velocity $\dot{\varphi}$ is set with a small electric motor. This motor acts in direction of ^3x_G and generates a torque of M_φ. A good compromise between output torque M_ψ and mechanical stability of the capability of roller bearings is an initial $\dot{\varphi}$ of $2500\ rad/s$.

The control of the torque M_θ has to take into account several constraints. As mentioned above the magnitude of the torque M_θ influences angular velocity $\dot{\theta}$ which has significant influence on the torque M_ψ. Next to the control of $\dot{\theta}$ the mean value of angle θ has to stay near zero over time. According to eq. (1) there is no torque output M_ψ for $\theta = \pi/2 + \pi \cdot x$, $x \epsilon \mathbb{Z}$. Though with an angle θ of $-\pi/2 < \theta < \pi/2$ the gyroscope stays predictable.

A suitable realization for the desired behavior of the inner gimbal is the fictive introduction of a spring and a damper mounted between inner and outer gimbal. So they react on the displacement of angle θ or angular velocity $\dot{\theta}$. Such a controller concept for torque M_θ is shown in [10]. In this disquisition the single output M_θ is controlled on a single input of the angle θ. The torque M_θ

$$M_\theta = c_{gyro}\theta + k_{gyro}\dot{\theta} \qquad (6)$$

with a spring constant of c_{gyro} and a damping constant of k_{gyro} is achieved. Another prospect for this controller concept is a PD-controller. The set point is angle θ and set to zero.

Depending on the magnitude of damping coefficient k_{gyro} the torque M_θ decelerates the inner gimbal on a precession induced displacement of the outer gimbal around angle ψ. The spring coefficient c_{gyro} generates an amount of M_θ keeping the displacement of $-\pi/2 < \theta < \pi/2$.

For the gyroscopic damper the values mentioned in Tab. 2 were found in an analysis and applied in the following examination.

Gyro Damper soft	$D_{gyro} = 0.25$
c_{gyro}	$-1\ [Nm/rad]$
k_{gyro}	$-4\ [Nm\ s/rad]$
Gyro Damper hard	$D_{gyro} = 0.5$
c_{gyro}	$-1\ \ [Nm/rad]$
k_{gyro}	$-1.6\ [Nm\ s/rad]$

Tab. 2:　　Damping and spring constants for torque controller M_θ.

The data of the quarter car model from Fig. 2 which is used for the further examination is shown in Tab. 3.

As introduced in [12] the quarter car for the vertical dynamic investigation has the following equation of motion for the vehicles body:

$$\ddot{z}_V = -\frac{k_{body}}{m_{sprung}}(\dot{z}_V - \dot{z}_T) - \frac{c_{body}}{m_{sprung}}(z_V - z_T) \qquad (7)$$

Equivalently the equation of motion for the tire is derived with

$$\ddot{z}_T\, m_{unsprung} = k_{body}(\dot{z}_V - \dot{z}_T) + c_{body}(z_V - z_T) - k_{tire}(\dot{z}_T - \dot{z}_S) \\ - c_{body}(z_T - z_S) \qquad (8)$$

The quarter car model is calculated in linear way. Therefore Tab. 3 presents the values in linear forces.

Since the damper force needs different damper constant for the body k_{body}, it is not defined in Tab. 3. In order to realize hard and soft damping behavior [12] defines the damping ratio Lehr with

$$D = \frac{k_{body}}{2\,\sqrt{c_{body}\,m_{sprung}}} \qquad (9)$$

An upper value for the damping ratio D is $D = 0.5$ and a lower value is $D = 0.25$ [12]. All further investigations in this paper compare the traditional linear damper with the gyroscopic damper on those two damping ratios. An equivalent k_{body} is calculated and provided in the simulation model.

m_{sprung}	400 $[kg]$
$m_{unsprung}$	40 $[kg]$
c_{body}	21 000 $[N/m]$
c_{tire}	150 000 $[N/m]$
k_{tire}	100 $[Ns/m]$

Tab. 3:   Data input for the quarter car (from [12] page 85).

The whole assembly shown in Fig. 1 was modelled as a multibody system using MapleSim [14]. The model of the quarter car from Fig. 2 was also included. The quarter car has the behavior of two oscillators. Afterwards the multibody system was embedded in a Matlab/Simulink [15] environment. This environment was chosen because Matlab/Simulink was considered as preferred software for controller implementation.

In the quarter car the torque M_{Damper} acting on the pivot of the lower wishbone can act as torque for a standard linear damper or the gyroscopic damper. The linear damper coefficient k_{body} acts as torque M_{Damper} with

$$M_{Damper} = k_{body} \left(\sin(\theta) \, l^2 + l \, \bar{z}_0 \right) \qquad (10)$$

In eq. (10) the length of the lower wishbone is defined as l and the spring preload is set with $\bar{z}_0$ such that the initial angle $\theta = 0$.

3 Results

Fig. 3 shows the results of the quarter car from Fig. 2 on a $5\,cm$ step input at z_S. In the diagram four different simulations are presented. The gyroscopic damper with a soft and a hard damping ratio is shown in continuous line. A linear damper with the same soft and hard damping ratio is shown in dashed lines. On the abscissa the simulation time is plotted. The three ordinates show the body heave z_V, the tire heave z_T and the dynamic tire force. Since the gyroscopic damper was controlled like mentioned in section 2 it shows almost the same behavior than the linear damper concept. Almost the same behavior of soft damping ratios (same for hard damping ratio) despite of different damping concepts allow a closer look on the characteristics of the gyroscopic damper.
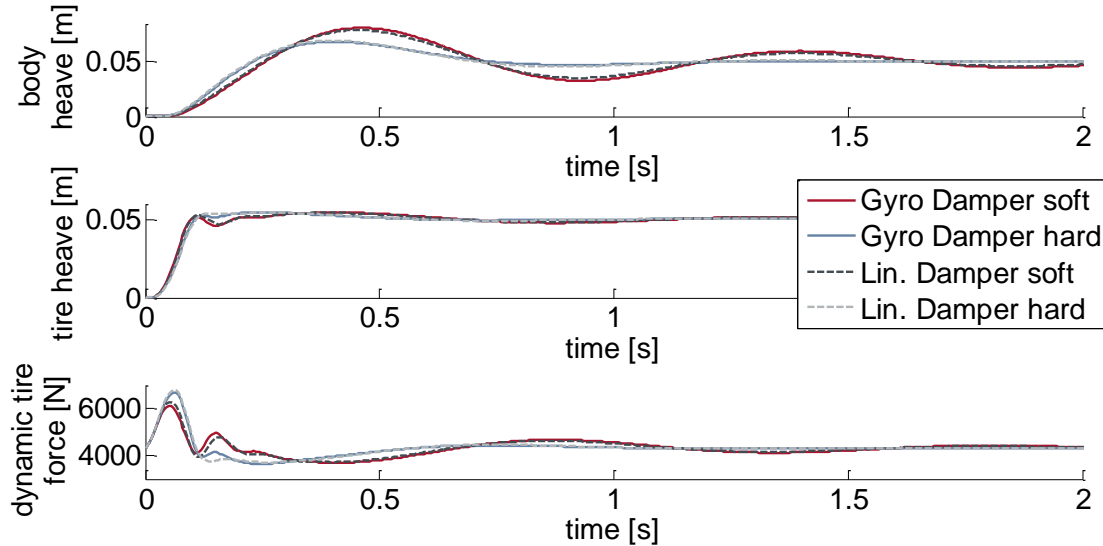

Fig. 3:   Simulation of a quarter car on $5\,cm$ step input as road displacement.

Fig. 4 shows the angle ψ and θ as well as the angular velocity $\dot{\varphi}$. Since the angle ψ is coupled to the pivot of the lower wishbone it simply follows its movement. Although the angle θ of the gyroscope is free it turns due to precession (compare section 2). The range for the angle θ satisfies $-\pi/2 < \theta < \pi/2$. This means we can trust the shown result with no singularity occurred.

Fig. 5 shows the torques M_{ψ}, M_{θ} and M_{φ}. The torque M_{φ} is equivalent to the damper torque M_{Damper}. Torque M_{θ} is the damping torque of the electric motor on axis θ.

One observation is the high quotient of $M_\psi / M_\theta \gg 1$. That means a small effort of M_θ results in a high damper torque. For this example the ratio is about $i \approx -570/19 = -30$ for the hard damper rate and about $i \approx -343/27 = -12$ for the soft damper rate. These different ratios between input and output torque can be compared to a gear box with a variable transmission ratio. The same ratio can be observed between $\dot\theta$ and $\dot\varphi$ which is not plotted.
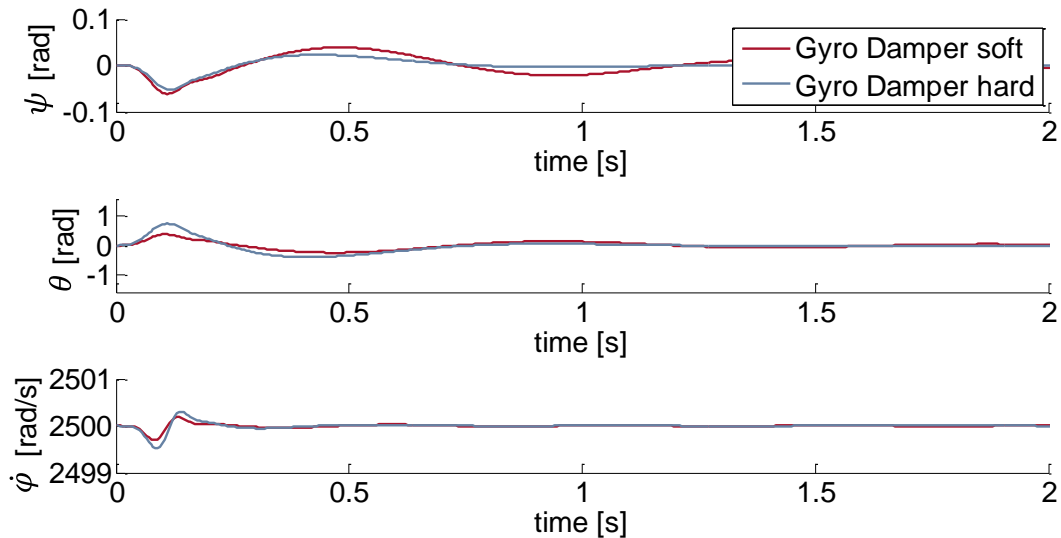

Fig. 4:   Behavior of the gyroscopic damper on $5\ cm$ step input as road displacement.
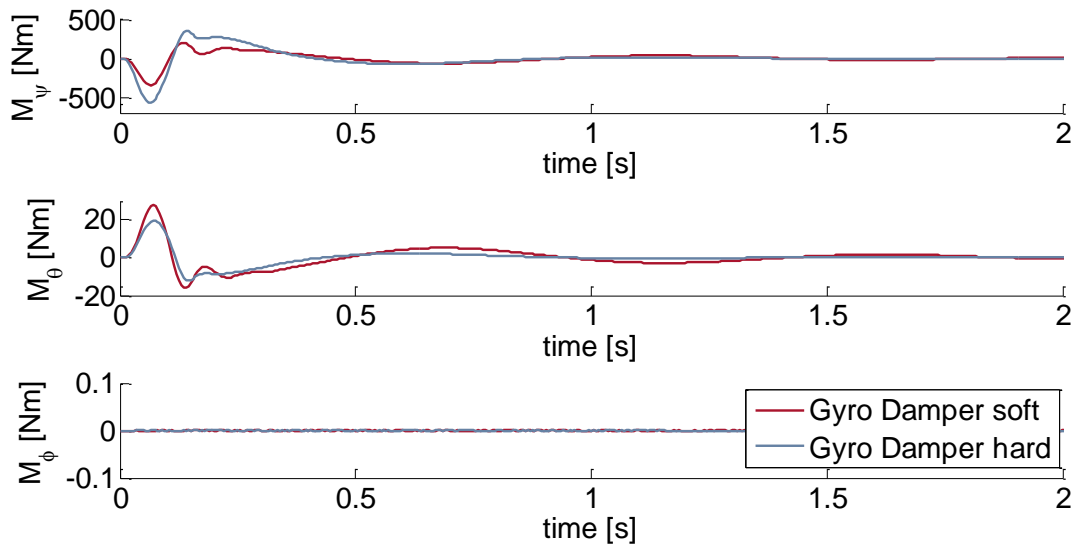

Fig. 5:   Torque input and torque output of the Gyro Damper on $5\ cm$ step input as road displacement.

Next examination considers a sweep input. It starts from an amplitude of $3\ cm$ with a frequency of $0.1\ Hz$ and ends in an amplitude of $1\ cm$ with a frequency of $15\ Hz$. This signal is the input at z_S. The results are shown in Fig. 6. On the abscissa the frequency is plotted. On the ordinate there is the transfer function of body heave acceleration over road displacement and the tire force over road displacement plotted. Over the whole frequency range the gyroscopic damper has the same

behavior like the linear damper. Slightly small differences can be observed especially in the tire force. Since the controller concept in order to control M_θ introduced in section 2 is a linear controller and the damper output M_ψ comprises non-linear terms (see eq. (4)) just a rough analysis is appropriate.

Symmetrical input as road displacement and a symmetrical damper coefficient of the gyroscopic damper are not a realistic application. Consequently on the one hand a stochastic road displacement from a measurement on a bad country road is applied. On the other hand an adjustable damping rate between hard and soft damper rate is used. According to a simple Skyhook control as shown in Tab. 4 the system switches between a hard and a soft damper rate.

$\dot{z}_V (\dot{z}_V - \dot{z}_T) > 0$	Damper hard
$\dot{z}_V (\dot{z}_V - \dot{z}_T) \leq 0$	Damper soft

Tab. 4:　　Applied Skyhook control according to [16].

This input for road displacement and the Skyhook control present a maximal asymmetric requirement on the gyroscopic damper. Nevertheless Fig. 7 shows the transfer functions for both the linear damper and the gyroscopic damper.
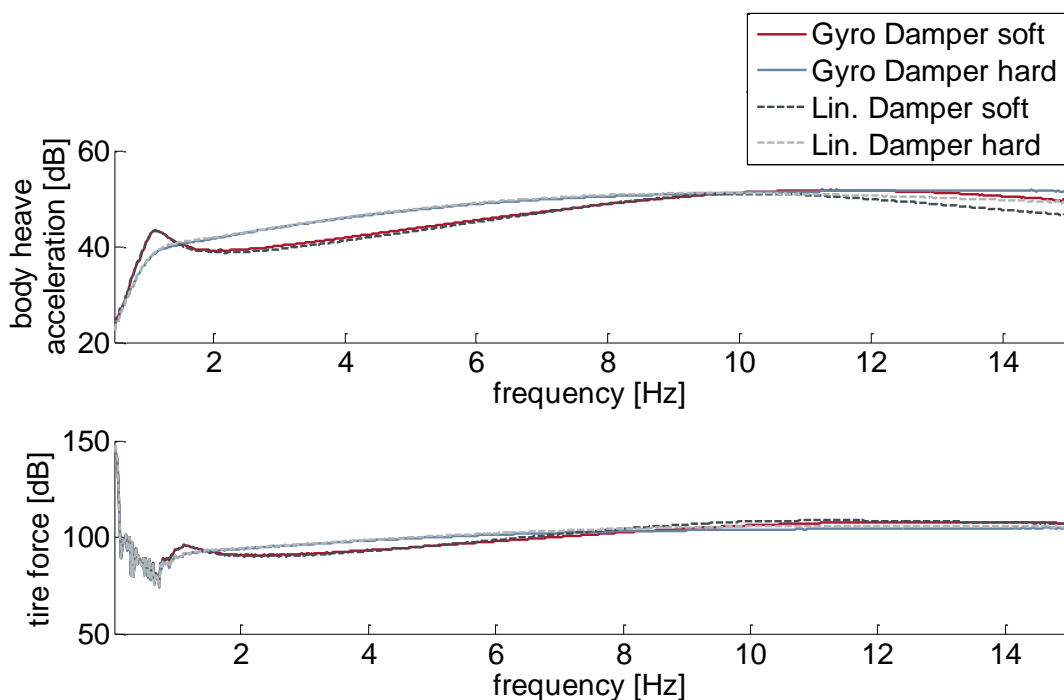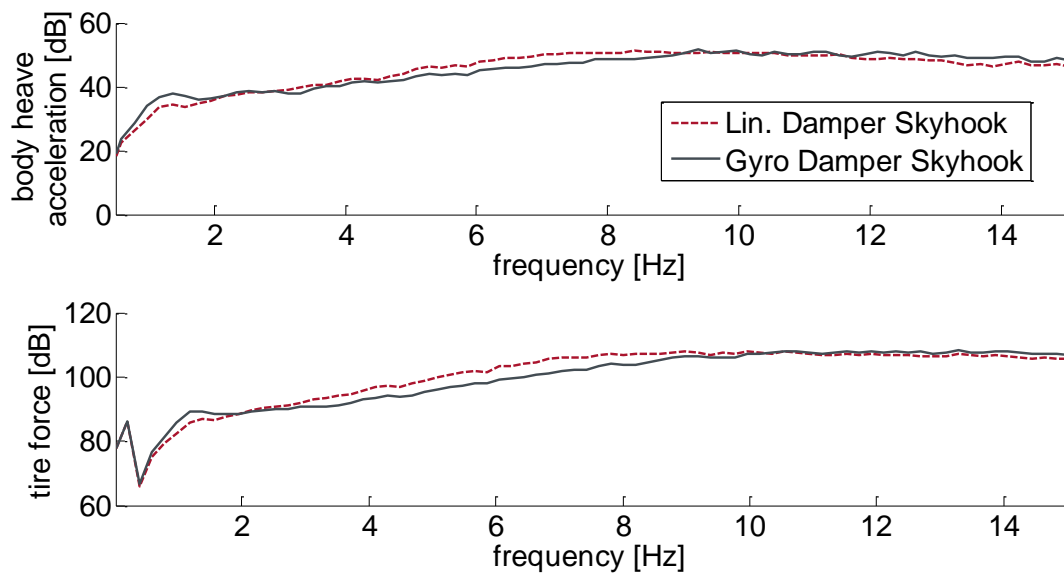

Fig. 6:　　Results on a sweep input.

Fig. 7:   Transfer function on stochastic street height with a Skyhook control.

Remarkable is the feasibility independent of both stochastic street input and stochastic torque request. There was no run away of the angle θ which means there was the capability to act with full torque potential at each moment.
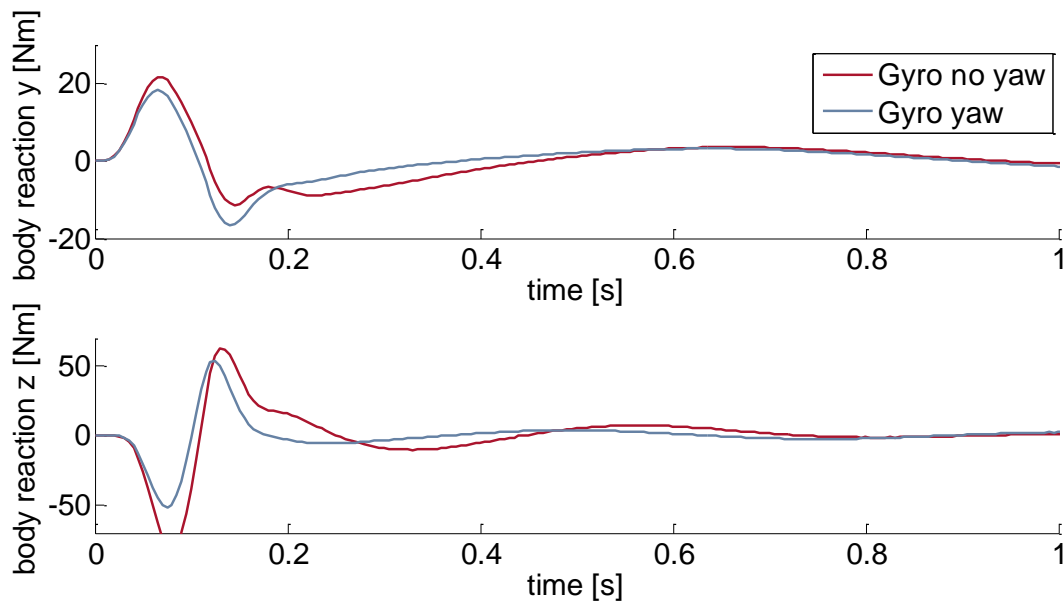

Fig. 8:   Behavior of the gyroscopic damper during yaw rate of the vehicle.

Since the gyroscope reacts on all angular velocities the next examination regards a yaw rate of the vehicle with $\dot{z}_V = 5 \, [rad/s]$. The same step input as road displacement from Fig. 3 leads to the behavior plotted in Fig. 8. The torque M_x is not shown because it is zero. The torque M_z shows the influence on the yaw behavior of the vehicle. The torque M_y has the same magnitude as the torque of the electric generator for the torque M_θ.

4   Discussion

Altogether over the whole spectrum of a passenger car's damping requirements the gyroscopic damper system seems to serve as an alternative. It was proven that the gyroscopic damper system manages all the situations which are required for application in a vehicle. A system with the same damping behavior than the standard telescopic damper concept legitimates itself with its sum of additional characteristics. As mentioned above there is the possibility to work with a different packaging. There is the capability to recuperate kinetic energy from the unevenness of the street. And there is the possibility to use the rotating system as kinetic energy storage. The recuperation of a stochastic road displacement allows the whole damper system to smooth the energy output to the car's on-board electrical system with the help of the inner electric motor torque M_φ.

Since the damper torque output M_ψ is almost zero if the angular velocity $\dot\theta$ is zero, it is very easy to realize a very soft damper behavior. This gives a potential of a high spread between soft and hard damper ratio.

Moreover the construction should avoid bad influence in yaw behavior. Even if the examination showed that the influence is not very high, possibilities to reduce certain behavior on a yaw rate should be analyzed. In a real car there will be four gyroscopic damper systems. Altogether they can divide themselves by different signs of $\dot\varphi$. This eliminates all torques around the yaw axis. Same procedure is conceivable for the reaction torque M_y.

As an outlook an optimized control concept for M_θ of the gyroscopic damper could create new possibilities. First a non-linear damping behavior resulting from sine and cosine terms in eq. (4) can be avoided. Second an optimization at high frequencies justify whether or not there is a possibility to reduce vibrations and to increase comfort. Third a bigger spread of a soft and a hard damper rate can be examined. In the end the torque M_θ could be controlled that $\ddot\varphi \neq 0$ resulting from the energy recuperation of the road displacement without the use M_φ.

5   References

[1]   ZUO, L.; ZHANG, P.-S.
      Energy Harvesting, Ride Comfort and Road Handling of Energy Regenerative
      Vehicle Suspensions
      Proceedings of 2011 ASME Vehicle Dynamic Systems and Control Conference
      USA, 2011

[2]   WILLEMS, M.
      Potenzialabschätzung zur Rekuperation der Stossdämpferenergie
      ATZ 09|2012 114. Jahrgang
      Germany, 2012

[3]   LI, Z.; ZUO L.; KUANG J.; GEORGE L.
      Energy Harvesting Damper with a Mechanical Motion Rectifier
      Smart Materials and Structures 21 December
      2012

[4]   WILLEMS, M.
      Chances and Concepts for Recuperating Damper Systems
      21st Aachen Colloquium Automobile and Engine Technology
      Aachen 2012

[5]   MOSSBERG, J.; ANDERSON, Z.; TUCKER, C.; SCHNEIDER, J.
      Recovering Energy from Damper Motion on Heavy Duty Commercial Vehicles
      SAE International
      2012

[6]   EBRAHIMI, B.; KHAMESEE, M. B.; GOLNARAGHI, M. F.
      Design and Modelling of a Magnetic Damper Based on Eddy Current Damping
      Effect
      Journal of Sound and Vibration
      2008

[7]   SALCEDO, F.; RUIZ-MINGUELA, P.; RODRIGUEZ, R.; et. al.
      Oceantec: Sea Trials of a Quarter Scale Prototype
      Proceedings of 8th European Wave Tidal Energy Conference
      Uppsala, Sweden, 2009

[8]   KANKI, H.; ARII, S.; FURUSAWA, T.; OTOYO, T.
      Development of advanced wave power generation system by applying
      gyroscopic moment
      Wave and Tidal Energy Conference
      2009

[9]   NISHIHARA, O.; MATSUHISA, H.
      Design Optimization of Passive Gyroscopic Damper
      JSME International Journal, Series C, Vol. 40, No. 4
      1997

[10] HAGHIGHI, H.; JAHED-MOTLAGH, M.;
      Ship Roll Stabilization via Sliding Mode Control and Gyrostabilizer
      Bul. Inst. Polit. Iasi, LVIII
      2012

[11] SCHRAMM, D.; HILLER, M.; BARDINI, R.
      Modellbildung und Simulation der Dynamik von Kraftfahrzeugen
      Springer Vieweg
      2013

[12] HEIßING, B.; ERSOY, M.; GIES, S.
      Fahrwerkhandbuch
      Vieweg und Teubner
      2011

[13] ASSMANN, B.; SELKE, P.
      Technische Mechanik 3
      Oldenbourg Verlag München Wien
      2007

[14] Maplesoft
      MapleSim
      Cybernet Systems Co., Ltd.
      Version 6.4, 2013

[15] MathWorks
      Matlab Simulink
      Version 2012b, 2012

[16] KARNOPP, D.; CROSBY, M. J.; HARWOOD, R. A.
      Vibration control using semi-active force generators
      ASME Journal of Engineering for Industry, 96:619–626
      1974